

ELEVENTH
INTERNATIONAL
SEMINAR



UNDER THE PATRONAGE OF



SAPIENZA
UNIVERSITÀ DI ROMA



**XI
INTERNATIONAL
SEMINAR
FIRE AND
EXPLOSION
HAZARDS**

ROME (ITALY)

June 15 – 20, 2025

Sapienza University of Rome



PROCEEDINGS

XI
INTERNATIONAL
SEMINAR

FIRE AND
EXPLOSION
HAZARDS



Proceedings of the Eleventh International Seminar on Fire and Explosion Hazards

15-20 June 2025, Rome, Italy

Edited by Paola Russo, Sapienza University of Rome

Maria Chiara Lancia, Sapienza University Rome

Copyright and Disclaimer

The papers published in the ISFEH 11 Proceedings are protected by copyright, which allows for subsequent publication elsewhere, but only in modified and extended form and with the full reference to the ISFEH 11 Proceedings.

All articles in the Proceedings have been peer reviewed. Neither of the editors shall be responsible for content of this publication. The editors do not guarantee the accuracy, correctness, or completeness of any content appearing in this publication of book of abstract and hence do not assume responsibility of any error or omissions arising from the use of this material.

<https://doi.org/10.5281/zenodo.16621853>

Rome, Italy

Sapienza University of Rome

2025

Neural network for real-time estimation of solid phase pyrolysis parameters

Lázaro D.^{1,*}, Lázaro M.¹, Alvear D.¹, Jiménez M.A.², Morgado, E.²

¹ *Universidad de Cantabria, Santander, Cantabria, Spain*

² *Consejo de Seguridad Nuclear, CSN, Madrid, Spain*

*Corresponding author email: lazarod@unican.es

ABSTRACT

The rate at which solid fuel is pyrolyzed is of great importance to determine combustion reaction rates at fires. As this transient process is highly sensitive on temperatures, the mass loss rate (MLR) tends to be derived by Arrhenius expression. Over the last decade years, novel optimization methodologies have emerged to obtain estimations of the thermokinetic parameters to simulate fire scenarios with the support of sophisticated models. While these works are based on different artificial intelligence techniques, they share a common approach: when the user need to study a specific material, they launch thousands of simulations to find an optimized set of parameters which fix the best with a dependent parameter, like the mass loss rate curve.

This study aims to define an inverse approach, training a neural network (NN), with thermokinetic parameters and thousands of mass loss rate simulations to create a single database, that once generated, can be applied to all subsequent analyses, reducing computational costs. Therefore, when one user needs to implement thermokinetic parameters in their fire engineering calculations, they must only supply the AI model with a MLR curve from bench-scale experiments, like gasification apparatus or Fire Propagation Apparatus (FPA). By processing this input, the corresponding reaction scheme and thermokinetic parameters are directly supplied.

To validate the proposed AI model, it was directly applied to ten gasification apparatus experimental MLR curves obtained from the Fire Dynamics Simulator (FDS) Validation Guide. The results showcased an improvement in the uncertainty parameters compared to the Guide, underscoring the potential of utilizing neural networks to enhance the accuracy of FDS simulations for solid-phase pyrolysis. The proposed AI model can characterize the materials in few seconds, making it a tool of great interest for obtaining the input parameters of the FDS model from experimental tests.

KEYWORDS: solid-phase pyrolysis; FDS; mass loss rate; neural network

INTRODUCTION

Kinetic parameters are essential for defining material reactions, but they cannot be directly measured. Traditionally, two main approaches have been used to estimate these parameters: analytical methods and curve-fitting optimization methods [1-2]. Analytical methods, such as model-fitting and model-free, rely solely on experimental results and are calculated independently from the computational model. On the other hand, curve-fitting optimization methods are efficient for complex processes involving multiple reactions, allowing not only the estimation of kinetic parameters but also the generation of reaction schemes and thermal properties that best fit the material in the desired computational model. However, these optimization methods require a significant computational effort, often involving thousands of simulations for each analysis [3].

Various researchers have explored different optimization algorithms to estimate material pyrolysis properties. Rein applied genetic algorithms (GA) to estimate material pyrolysis properties from thermogravimetric analysis (TGA)[4] and cone calorimeter experiments [5]. Lautenberger developed the computational model Gpyro [6], which allows users to automatically execute optimization algorithms for estimating material pyrolysis properties. Matala used genetic algorithms to estimate pyrolysis modeling parameters for PVC cables using TGA and cone calorimeter tests [7]. Webster applied a stochastic hill climber method to obtain material pyrolysis properties from cone calorimeter experiments, concluding that it provides better performance than GA [8]. Additionally, Ghorbani

performed optimization with cone calorimeter tests using GA and SHC algorithms [9]. Chaos employed shuffled complex evolution (SCE) optimization, achieving better results than GA for extracting material pyrolysis properties from FPA experiments [10-11]. Alonso used SCE to optimize TGA and differential scanning calorimetry experimental tests to obtain kinetic properties of linear low-density polyethylene for the FDS model [12]. Hehnen also employed an SCE algorithm on the results of experimental tests from micro-scale calorimeter and cone calorimeter to obtain the parameters that define a material in FDS [13]. Nevertheless, the process of estimating typical material pyrolysis properties still demands the execution of tens of thousands of trial solutions, consuming several hours even on high-performance 16-core computer clusters [3].

Given this context, there is a clear need for the development of a novel methodology that enables the instantaneous characterization of material solid-phase pyrolysis and its specific definition within a computational model. Such a methodology would eliminate the requirement of conducting numerous simulations for each analysis.

This study aims to enhance the accuracy of FDS simulations by using a neural network to estimate, in real-time, the reaction scheme and thermokinetic parameters for defining solid-phase pyrolysis. The artificial intelligence model developed was trained with FDS simulations to ensure its applicability for this computational model. For this purpose, a total of 245,700 simulations were executed to facilitate the training of the neural networks. Subsequently, the AI model will be supplied with an experimental MLR curve obtained in a bench-scale test performed under a nitrogen atmosphere to analyse pyrolysis. By processing this input, the AI model will generate, in real-time, the corresponding reaction scheme and thermokinetic parameters necessary for defining the solid-phase pyrolysis. The proposed AI model is validated with 10 MLR experimental curves taken from the FDS Validation Guide[14] to obtain the reaction scheme and the thermokinetic parameters. The results of this study show the potential of using neural networks to improve the accuracy of FDS simulations for the solid-phase pyrolysis of polymeric materials.

METHODS

This section describes the neural network architecture employed in the developed AI model and the definition of the training data. The neural network employed in the model is a General Regression Neural Network (GRNN) [15] which is often used for function approximation. GRNN is a variant of the radial basis function neural network and is a powerful tool for nonlinear function approximation [16]. The GRNN used in this study is defined in MATLAB [17], and it consists of a radial basis layer with a special linear layer, as shown in Fig. 1.

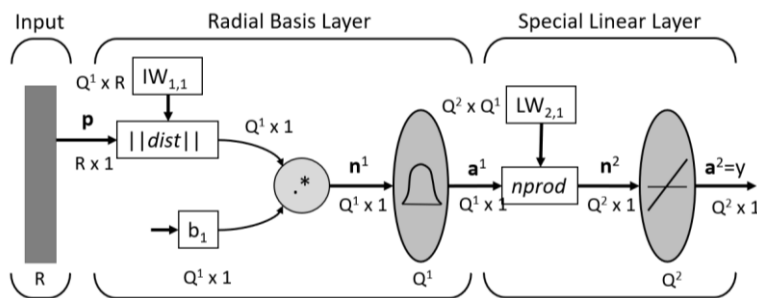


Fig. 1. GRNN architecture.

Where R is the number of elements in the input vector (p), Q^1 the number of neurons in layer 1, Q^2 the number of layers of layer 2, and y the output vector. The radial basis layer of the network comprises R neurons. The bias vector, b_1 , is set to 0.8326 divided by the user-defined parameter, SPREAD. SPREAD determines the distance at which an input vector must be from a neuron's weight vector for the output to reach 0.5. A larger SPREAD results in a larger response area for layer 1

neurons around the input vector and a smoother network function with multiple neurons contributing to the output. Conversely, a small SPREAD results in a steeper radial basis function with a higher output from the neuron closest to the input vector. Default SPREAD value is 1.0.

In the network, the weighted input of each neuron is calculated as the Euclidean distance between the input vector and its first-layer input weights using the MATLAB function "dist". The net input of each neuron is obtained by multiplying its weighted input with its bias, computed using the operator "*". The output of each neuron is obtained by passing its net input through the MATLAB function "radbas" (Fig.2). If a neuron's weight vector is equal to the input vector (transposed), the weighted input becomes 0, resulting in a net input of 0 and an output of 1. If a neuron's weight vector is located at a distance of SPREAD from the input vector, it will result in an output of 0.5.

The second layer of the network comprises the same number of neurons as the input vectors. The MATLAB function "nprod" calculates the dot product of each row of the second-layer weights (LW2,1) with the input vector a^l , normalized by the sum of elements in a^l , resulting in a vector n^2 . Finally, linear transfer function "purelin" is used to obtain output y .

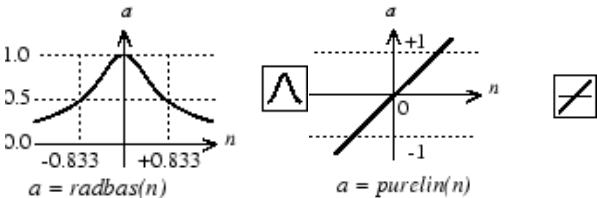


Fig. 2. Radial Basis and linear Transfer Functions. [17]

Through the training, the neural network learns to associate specific MLR curves with the pyrolysis reaction scheme and thermokinetic parameters. For the training, the FDS gasification apparatus definition is based on the outlined in the FDS User Guide [18]. These tests focus solely on solid-phase pyrolysis, disabling all gas-phase computations to accelerate the simulation. However, convective heat transfer to and from the surface is still considered, using the ambient temperature. An incident heat flux of 50 kW/m² was uniformly applied to the sample surface for all training simulations.

The training process is organized based on the type of reaction and the sample thickness. Each pair of reaction and thickness corresponds to a specific neural network, making the training for each case independent. Table 1 collects the different reactions and thicknesses used for the training of the AI model, enabling the AI model to analyze them.

Table 1. Cases analyzed by the AI model

Reactions	1 without char	1 with char	2 without char	2 with char
Thickness (mm)	4,5,6,1,7,8,9,10			

Table 2 presents the thermokinetic parameters and their corresponding range of variation used in defining the training simulations. This range is valid for the virgin material, and, for the intermediate material and the char (in case of two reaction, with/without char). The range of each parameter is large enough to consider variations between different materials and state of the material during the decomposition[14]. A total of 245,700 simulations were executed to facilitate the training of the neural networks. Consequently, 28 neural networks were developed, one for each thickness and type of reaction.

While an initial attempt to create a global neural network covering all thicknesses and reaction schemes yielded unsatisfactory results, an alternative approach, dividing the problem into different neural networks, significantly improved accuracy. The better performance of considering separated neural networks relies in the weight of each training input parameters, each associated initially with a neuron. To consider a global neural network, the neural network training input parameters should consider not only the MLR values, but also the thickness and reaction type. Nevertheless, as the model

analyses as training input parameters 40 MLR values (as the MLR curve is discretized into 40 temporal instants), the significance and influence in the results of the thickness and reaction type is only the 2.4 %, while actually, these parameters have a huge influence on the decomposition. Subsequently, when a user selects a specific thickness, only four neural networks (one per reaction scheme) will be employed in each analysis, ensuring efficient and rapid model performance, generating results within a few seconds.

Table 2. FDS input parameters for the definition of the training simulations

Input parameters	Range	Input parameters	low
Emissivity	[0.85-0.97]	Activation energy (kJ/kmol)	[100000-360000]
Thermal conductivity (W/m/K)	[0.1-0.4]	Absorption coef. (m-1)	[500-5000]
Specific heat (kJ/kg/K)	[1.0-4.0]	Heat of reaction (kJ/kg)	[700-2000]
Reaction order (-)	[0.7-1.5]	Initial density (kg/m3)	[800-1500]
Preexponential factor (1/s)	[1E+10-1E+24]	Percentage of char	[0.05-0.95]

Once the neural network architecture was chosen, and the training data was obtained through simulations, the next step involved integrating the model into a tool to facilitate automation of the analysis. Fig. 3 illustrates the overall structure of the model, encompassing the training process, network definition, validation of the model and its final use. As it is included in the Fig. 3, the training has been performed with computational simulations, and the validation with experimental tests. It should be noted that the “Trained Neural Network” and the “Validated Neural Network” of the Fig. 3 are the same, as validation does not produce any internal variation in the neural network.

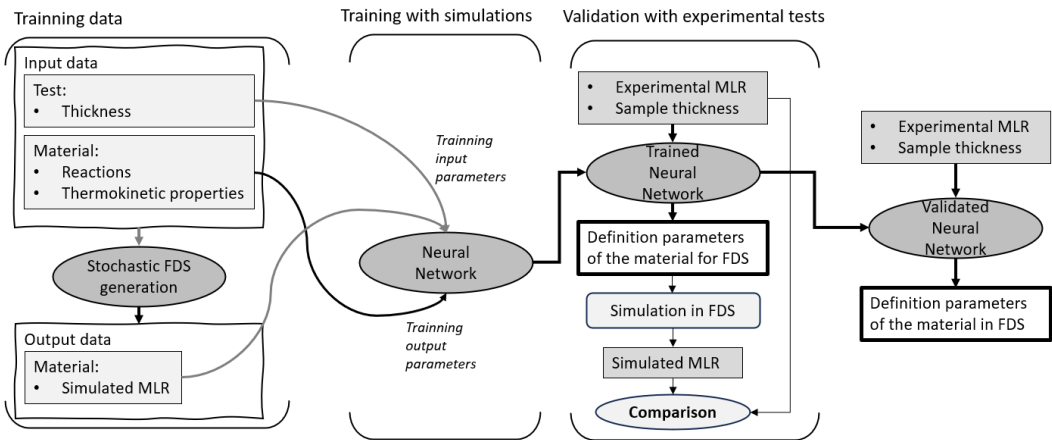


Fig. 3. Scheme of the integrated tool.

The sample thickness will be selected by the user based on the thickness used in the experimental test to be analyzed. The AI model will then assess which reaction scheme provides a better fit to the experimental MLR data. The experimental MLR curves has to be obtained from gasification apparatus or FPA tests conducted under an inert atmosphere. To achieve accurate results, it is essential to conduct the experimental tests under an external incident heat flux of 50 kW/m². Then, the model will provide the thermokinetic parameters to define the pyrolysis model in FDS. These parameters are the ones collected in the Table 2.

To conduct this assessment, four independent neural networks have been defined, one for each reaction scheme. The model will obtain the thermokinetic parameters for each reaction scheme and perform four simulations in FDS, evaluating the best adjustment for each set of parameters. These simulations yield results within a few seconds, allowing for quick and efficient analysis. Ultimately,

the reaction scheme and thermokinetic parameters that best fit the experimental data will be identified and retained.

VALIDATION RESULTS

To perform the validation of the developed model, it was applied to ten experimental tests conducted in the NIST gasification apparatus under a nitrogen atmosphere. These experimental tests were collected from the FDS Validation Guide [14] and involved different polymers. All tests were conducted with an incident heat flux of 50 kW/m². Table 3 provides details of the tested polymers and their respective thicknesses. The results obtained from the AI model will include the thermokinetic parameters and the reaction scheme for each material.

For each material, the figures will present a comparison between the experimental MLR curve and the MLR obtained from the FDS model using the AI model's material definition. In all figures, the experimental test results will be represented by black lines, the AI model results with red lines and the FDS validation guide results with grey lines.

Table 3. Materials analyzed with the model and their thicknesses

Material	Thickness	Material	Thickness
PA66	6.1 mm	HDPE	9mm
Kydex	6.1 mm	PBT	4mm
PET	6.1 mm	PBT-GF	4mm
PP	6.1 mm	HIPS	6mm
POM	6.1 mm	HIPS	9mm

For each case of study, the Mean Square Error (MSE) has been evaluated using the following equation:

$$MSE = \frac{1}{n} \sum_{i=1}^n (E_i - M_i)^2 \quad (1)$$

Where n is the total number of time instants in the MLR curves, E_i is the experimental MLR result at time instant i , and M_i is the simulated MLR result at time instant i . Time instants multiples of 20 s have been evaluated. By squaring the errors, we ensure that the error values are always positive, and a perfect match results in an error of 0. If we did not square the error, the values could be positive or negative, causing potential issues when analyzing the overall accuracy. To provide a more intuitive error value, the Root Mean Square Error (RMSE) is also employed in the analysis. RMSE is calculated by taking the square root of the MSE.

To organize the results, they have been clustered based on the number of reactions and char formation predicted by the AI model for each material. First, we present the results for a reaction scheme consisting of two decomposition reactions with char formation.

This is the case for the analyzed polyamide 6.6 (PA66) and Kydex materials. Both samples were tested using the NIST Gasification Apparatus with a thickness of 6.1 mm for each. Table 4 displays the parameters obtained by the AI model to define the decomposition reactions of PA66 and Kydex in FDS. The AI model predicted the following reaction schemes for PA66 and Kydex:

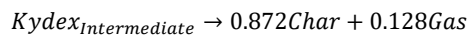
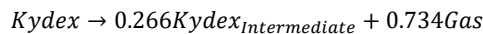
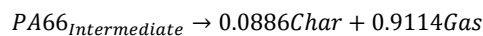


Table 4. Parameters obtained with the AI model for the PA6.6 and for the Kydex

Parameters	Reaction	AI model PA 66	AI model Kydex	Reaction	AI model PA 66	AI model Kydex
Density (kg/m ³)	r1	1320.0	1411.6	r2	172.4	375.2
Emissivity		0.9293	0.887		0.8679	0.884
conductivity (W/mK)		0.3183	0.318		0.2761	0.289
Specific Heat (kJ/kgK)		3.3466	1.450		2.3333	3.798
Reaction order		0.9941	1.229		0.9862	1.465
Preexponential factor (1/s)		9.10E+18	1.32E+12		3.22E+22	1.84E+16
Activation energy (kJ/kmol)		2.62E+05	1.25E+05		1.96E+05	2.05E+05
Absorption coeff. (1/m)		3.57E+03	1.83E+03		626.33	4.04E+03
Heat of reaction (kJ/kg)		852.90	1997.10		1.61E+03	1388.00
Relative amount of solid product		0.1306	0.266		0.0886	0.872
Density (kg/m ³)	char	15.3	327.05			
Emissivity		0.7381	0.594			
conductivity (W/mK)		1.7433	0.631			
Specific Heat (kJ/kgK)		4.3108	5.332			
Absorption coeff. (1/m)		441.67	3.03E+03			

Figure 4 illustrates the comparison of the PA66 MLR curve obtained in FDS using the parameters provided by the AI model against the MLR curve obtained by the original parameters found in FDS Validation Guide and against the experimental results. It is evident that the neural network successfully approximates the MLR curve of PA6.6, accurately capturing the growth and decay phases, and closely resembling the peak value observed in the experimental data. The performance metrics for this case indicate an MSE of 4.34E-06 and an RMSE of 0.0021 kg/sm² for the AI model, and an MSE of 1.20E-05 and an RMSE of 0.0035 kg/sm² for the simulation included in the FDS Validation Guide.

Moving on to the Kydex material, Figure 5 displays the comparison of the Kydex MLR curve obtained in FDS using the parameters generated by the AI model with the simulated curve included in the FDS Validation Guide. The adjustment made by the proposed AI model results in a well-fitting MLR curve. For this case, the proposed model achieves an MSE of 3.22E-06 and an RMSE of 0.0018 kg/sm², while an MSE of 1.73E-05 and an RMSE of 0.0042 kg/sm² for the simulation included in the FDS Validation Guide.

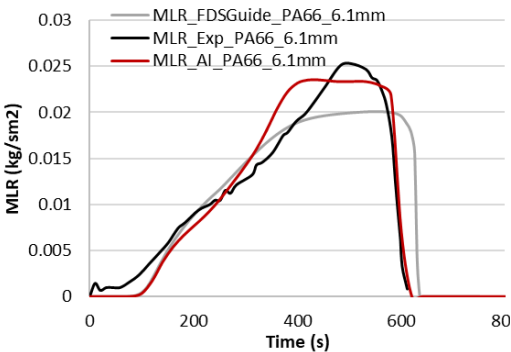


Fig. 4. Comparison of the PA6.6 MLR curves.

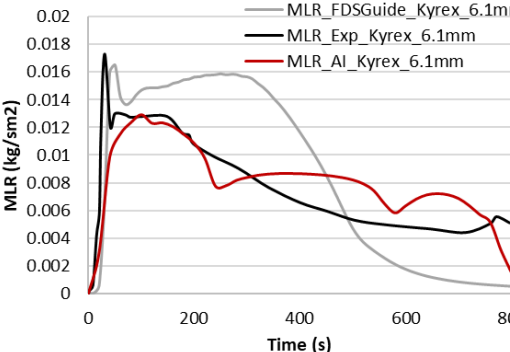
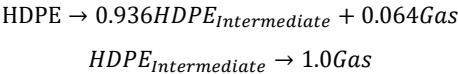


Fig. 5. Comparison of the Kydex MLR curves.

Now, the materials analyzed by the AI model with a decomposition scheme of two reactions without the formation of residue are presented. This includes high-density polyethylene (HDPE) and polybutylene terephthalate with glass fibers (PBT-GF). The AI model successfully predicted the reaction schemes for HDPE and PBT-GF, which are shown below:



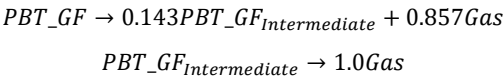


Table 5. Parameters obtained with the AI model for the HDPE and for the PBT-GF

Parameters	Reaction	IA model HDPE	IA model PBT-GF	Reaction	IA model HDPE	IA model PBT-GF
Density (kg/m ³)	r1	949.67	993.36	r2	888.521	142.07
Emissivity		0.922	0.920		0.891	0.883
conductivity (W/mK)		0.369	0.136		0.235	0.248
Specific Heat (kJ/kgK)		1.848	2.028		1.362	1.849
Reaction order		0.709	1.260		0.924	0.952
Preexponential factor (1/s)		3.55E+13	1.18E+20		7.67E+18	5.59E+13
Activation energy (kJ/kmol)		1.32E+05	2.78E+05		2.36E+05	1.06E+05
Absorption coeff. (1/m)		829.09	5.09E+02		1.03E+03	1.05E+03
Heat of reaction (kJ/kg)		1.60E+03	1461.00		827.18	1834.70
Relative amount of solid product		0.936	0.143		0.00	0

Figure 6 depicts the comparison of the HDPE MLR curves, obtained in FDS using the parameters derived from the AI model, the ones of the FDS Validation Guide and the experimental MLR curve. While the peak value obtained by the AI model is slightly higher than the experimental one, the peak decay instant is accurately represented. The performance metrics for this case indicate an MSE of 2.58E-05 and an RMSE of 0.0051 kg/sm² for the AI model, and an MSE of 5.80E-05 and an RMSE of 0.0076 kg/sm² for the simulation included in the FDS Validation Guide.

Subsequently, Figure 7 illustrates the comparison of the PBT-GF MLR curves obtained in FDS with the experimental MLR curve. The proposed AI model achieves a good fit, with an MSE of 1.48E-06 and an RMSE of 0.0012 kg/sm², while an MSE of 6.31E-06 and an RMSE of 0.0025 kg/sm² were obtained for the simulation included in the FDS Validation Guide.

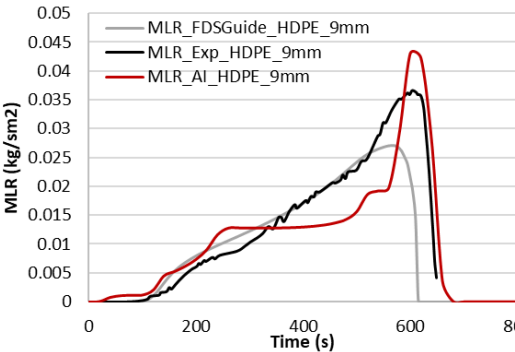


Fig. 6. Comparison of the HDPE MLR curves.

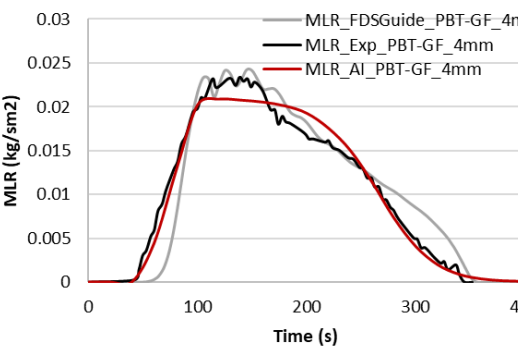


Fig. 7. Comparison of the PBT-GF MLR curves.

Finally, we present the materials with a decomposition scheme consisting of just one reaction without char formation. The materials analyzed in this category and their corresponding predicted thermokinetic properties are included in Table 6.

Table 6. Parameters obtained with the AI model for the materials with one reaction

Parameters	IA model PET (6.1mm)	IA model PP (6.1mm)	IA model POM (6.1mm)	IA model PBT (4mm)	IA model HIPS (6mm)	IA model HIPS (9mm)	IA model ABS (6.4mm)
Density (kg/m ³)	1159.50	867.60	1492.50	1152.70	1009.90	985.94	1077.70
Emissivity	0.917	0.867	0.903	0.896	0.861	0.959	0.941
Conductivity (W/mK)	0.198	0.218	0.214	0.359	0.208	0.167	0.202

Specific Heat (kJ/kgK)	2.529	3.847	2.973	3.565	1.642	2.198	3.050
Reaction order	0.704	1.221	1.202	1.100	0.956	0.940	0.735
Preexponential factor (1/s)	3.85E+20	9.91E+14	5.30E+23	7.67E+21	5.35E+12	7.18E+17	2.90E+20
Activation energy (kJ/kmol)	2.99E+05	2.27E+05	3.06E+05	2.57E+05	1.87E+05	2.58E+05	2.17E+05
Absorption coeff. (1/m)	623.59	2.23E+03	2.79E+03	2.51E+03	1.69E+03	3.05E+03	9.90E+02
Heat of reaction (kJ/kg)	705.02	981.30	1624.80	741.31	1919.10	1295.10	1988.20

Firstly, in Figure 8, we observe the comparison of the polyethylene terephthalate (PET) MLR curve obtained in FDS with the parameters derived from the AI model, as previously shown in Table 6. Despite the predicted peak value being lower, the AI model effectively captures the growing and decreasing phases of the PET decomposition and accurately estimates the area under the MLR curve, which represents the total mass consumed. In this case, the AI model improve significantly the results compared to the ones of the FDS validation guide. For this case, the MSE of the proposed model is 7.14E-05, and the RMSE is 0.0085 kg/sm² for the AI model, and an MSE of 2.54E-04 and an RMSE of 0.0159 kg/sm² for the simulation included in the FDS Validation Guide.

Moving on to Figure 9, it presents the comparison of the polypropylene (PP) MLR curve obtained in FDS with the parameters obtained from the AI model, the ones of the FDS Validation Guide and the experimental MLR data. The AI model successfully generates parameters that result in a good approximation of the growing phase and the peak. In this instance, the MSE of the proposed model is 2.37E-05, and the RMSE is 0.0049 kg/sm² for the AI model, and an MSE of 2.65E-05 and an RMSE of 0.0051 kg/sm² for the simulation included in the FDS Validation Guide.

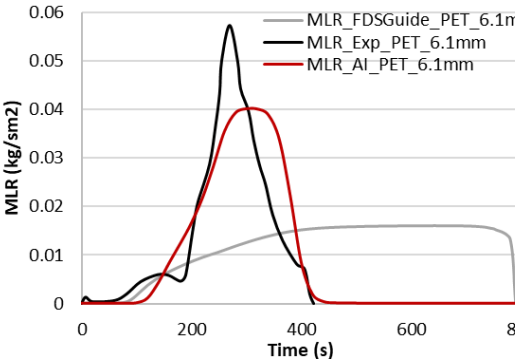


Fig. 8. Comparison of the PET MLR curves.

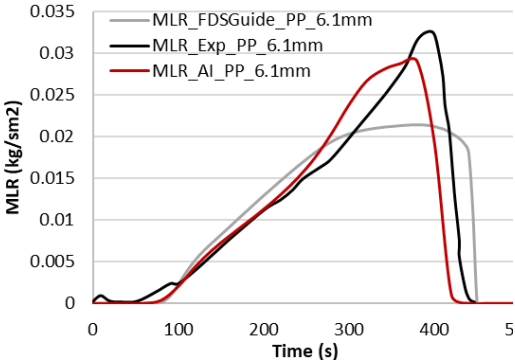


Fig. 9. Comparison of the PP MLR curves.

Figure 10 illustrates the comparison of the polyoxymethylene (POM) MLR curve obtained in FDS with the parameters derived from the AI model, as previously shown in the table. The figure demonstrates how the model effectively predicts the experimental curve. For this case, the MSE of the proposed model is 1.20E-05, and the RMSE is 0.0035 kg/sm² for the AI model, and an MSE of 1.61E-05 and an RMSE of 0.0040 kg/sm² for the simulation included in the FDS Validation Guide.

Subsequently, Figure 11 showcases the comparison of the polybutylene terephthalate (PBT) MLR curve obtained in FDS with the parameters obtained from the AI model in comparison to the ones of the FDS Validation Guide and the experimental result. The AI model successfully predicts the growing and decreasing phases, although the peak value is slightly lower than in the experimental test. In this instance, the MSE of the proposed model is 1.99E-05, and the RMSE is 0.0045 kg/sm² for the AI model, and an MSE of 1.08E-04 and an RMSE of 0.0104 kg/sm² for the simulation included in the FDS Validation Guide.

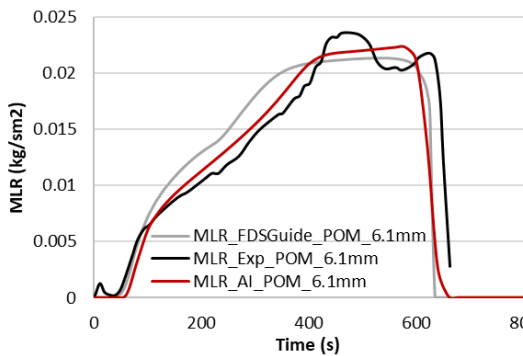


Fig. 10. Comparison of the POM MLR curves.

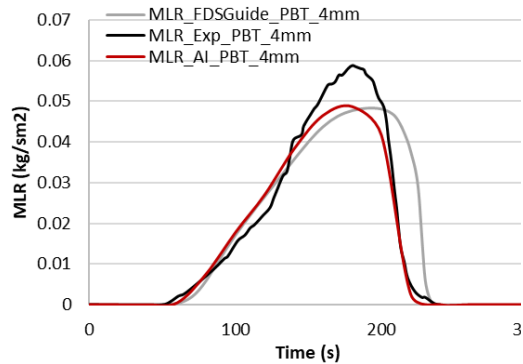


Fig. 11. Comparison of the PBT MLR curves.

Figure 12 presents the comparison of the MLR curve of high impact polystyrene (HIPS) with a thickness of 6 mm, obtained in FDS, with the parameters generated by the AI model, alongside the experimental test results. The AI model provides a material definition that effectively fits the experimental curve. For this case, the MSE of the proposed model is 1.19E-06, and the RMSE is 0.0011 kg/sm² for the AI model, and an MSE of 1.74E-05 and an RMSE of 0.0042 kg/sm² for the simulation included in the FDS Validation Guide.

Furthermore, in Figure 13, we observe the comparison of the MLR curve of HIPS with a thickness of 9 mm, obtained in FDS, with the parameters obtained from the AI model. The AI model correctly approximates the MLR curve of the 9 mm HIPS sample. In this instance, the MSE of the proposed model is 2.18E-06, and the RMSE is 0.0015 kg/sm² for the AI model, and an MSE of 1.97E-06 and an RMSE of 0.0014 kg/sm² for the simulation included in the FDS Validation Guide.

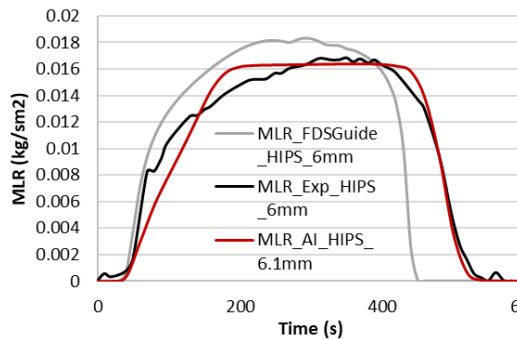


Fig. 12. Comparison of the HIPS 6 mm MLR curves.

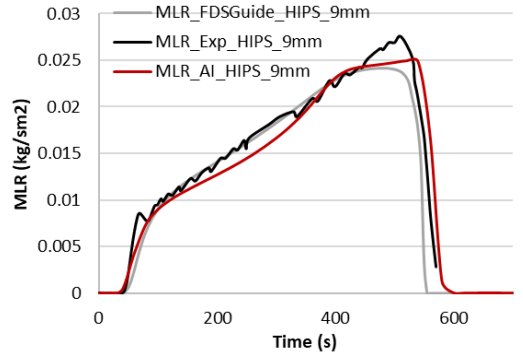


Fig. 13. Comparison of the HIPS 9 mm MLR curves.

Table 7 shows the MLR peak values for the cases analyzed in the direct application of the AI model. The MLR peak values of the simulations included in the FDS Validation Guide are also included. These values have been used to calculate the uncertainty of the proposed methodology.

Table 7. Comparison of the experimental and model MLR peak value for the different cases

Sample	Max MLR exp (kg/sm ²)	Max MLR AI mod (kg/sm ²)	Max MLR FDSGuide (kg/sm ²)
PA66_6.1mm_N2_50kW/m ²	0.0253	0.0235	0.0201
Kydex_6.1mm_N2_50kW/m ²	0.0173	0.0129	0.0165
PET_6.1mm_N2_50kW/m ²	0.0572	0.0401	0.0161
PP_6.1mm_N2_50kW/ m ²	0.0325	0.0290	0.0214

POM_6.1mm_N2_50kW/ m ²	0.0236	0.0223	0.0214
HDPE_9mm_N2_50kW/ m ²	0.0366	0.0431	0.0271
PBT_4mm_N2_50kW/ m ²	0.0588	0.0487	0.0484
PBT-GF_4mm_N2_50kW/ m ²	0.0234	0.0209	0.0243
HIPS_6mm_N2_50kW/ m ²	0.0169	0.0164	0.0184
HIPS_9mm_N2_50kW/ m ²	0.0276	0.0249	0.0242

Considering the MLR peaks it is calculated the MSE for the AI model and for the simulations of the FDSGuide versus the experimental value, obtaining 4.87E-05 and 2.06E-04 respectively. Additionally the RMSE for the comparison of AI model versus experimental results is of 6.98E-03 kg/ms² and for the comparison of the FDSGuide simulations versus experimental results of 1.43E-02 kg/ms².

CONCLUSIONS

In this paper, we have introduced a novel methodology to instantaneously characterize solid-phase pyrolysis of materials and define them for specific computational modeling. The key innovation lies in the utilization of a neural network trained with FDS simulations to estimate, in real-time, the input parameters required for accurate solid-phase pyrolysis modeling.

The validation of the proposed AI model was carried out by applying it to 10 MLR experimental curves of different materials. Our results showcased a substantial improvement in RMSE of the AI model proposed while comparing with the experimental tests compared to values provided in the FDS Validation Guide, with the RSME decreasing from 1.43E-0.2 kg/ms² in the Guide to 6.98E-03 kg/ms² in the AI model simulations.

The innovative methodology we presented exhibits the potential to significantly enhance the accuracy of FDS simulations for solid-phase pyrolysis of materials while reducing the need for an extensive number of simulations in each case. Currently, the model can analyze gasification apparatus or FPA tests under a heat flux of 50 kW/m² and a nitrogen atmosphere, for sample thicknesses ranging from 4 mm to 10 mm.

In conclusion, our proposed AI-based approach offers promising results for instantaneously characterizing solid-phase pyrolysis and defining materials for computational modeling. By providing more accurate and efficient simulations, this methodology paves the way for enhanced fire safety assessments and enables faster and more reliable analysis of material behavior in fire scenarios.

ACKNOWLEDGEMENTS

The authors would like to thank the Consejo de Seguridad Nuclear for the cooperation and co-financing of the project “Análisis de modelos numéricos y experimentales para la investigación de incendios en centrales nucleares” (FIRENUC) and for the research project SUBV-18/2022 “NUCLEVS - Validación, calibración y aplicación de modelos de propagación de incendios en escenarios reales de Centrales Nucleares”.

REFERENCES

- [1] A. Witkowski, A. A. Stec and T. R. Hull, “Chapter 7. Thermal decomposition of polymeric materials,” in *SFPE Handbook of Fire Protection Engineering, Fifth Edition*, SFPE, Ed., DOI 10.1007/978-1-4939-2565-0, 2016.
- [2] D. Lázaro, A. Alonso, M. Lázaro and D. Alvear, “A Simple Direct Method to Obtain Kinetic Parameters for Polymer Thermal Decomposition,” *Applied Sciences*, vol. 11(23), no. <https://doi.org/10.3390/app112311300>, 2021.

- [3] C. Lautenberger and A. C. Fernandez-Pello, "Optimization algorithms for material pyrolysis property estimation," *Fire Safety Science*, vol. 10, pp. 751-764, 2011.
- [4] G. Rein, C. Lautenberger, A. Fernandez-Pello, J. Torero and D. Urban, "Application of Genetic Algorithms and Thermogravimetry to Determine the Kinetics of Polyurethane Foam in Smoldering Combustion," *Combustion and Flame*, vol. 146, no. <http://dx.doi.org/10.1016/j.combustflame.2006.04.013>, pp. 95-108, 2006.
- [5] C. Lautenberger, G. Rein and A. Fernandez-Pello, "The Application of a Genetic Algorithm to Estimate Material Properties for Fire Modeling from Bench-Scale Fire Test Data," *Fire Safety Journal*, vol. 41, no. <http://dx.doi.org/10.1016/j.firesaf.2005.12.004>, pp. 204-214, 2006.
- [6] C. Lautenberger, "A Generalized Pyrolysis Model for Combustible Solids," Dissertation Doctor of Philosophy, University of California, Berkeley , 2007.
- [7] A. Matala and S. Hostikka, "Pyrolysis Modelling of PVC Cable Materials," in *Fire Safety Science- Proceedings of the tenth international symposium*, 2011.
- [8] R. Webster, M. Lázaro, D. Alvear, J. Capote and A. Trouvé, "Limitations in Current Parameter Estimation Techniques for Pyrolysis Modeling," in *Sixth Fire and Explosion Hazards Seminar (FEH6)* , 2010.
- [9] Z. Ghorbani, R. Webster, M. Lázaro and A. Trouvé, "Limitations in the predictive capability of pyrolysis models based on a calibrated semi-empirical approach," *Fire Safety Journal*, vol. 61 , no. <http://dx.doi.org/10.1016/j.firesaf.2013.09.007>, p. 274–288, 2013.
- [10] M. Chaos, M. Khan, N. Krishnamoorthy, J. de Ris and S. Dorofeev, "Bench-scale flammability experiments: determination of material properties using pyrolysis models for use in CFD fire simulations," in *Interflam* , 2010.
- [11] M. Chaos, M. M. Khan, N. Krishnamoorthy, J. L. de Ris and S. B. Dorofeev, "Evaluation of optimization schemes and determination of solid fuel properties for CFD fire models using bench-scale pyrolysis tests," *Proceedings of the Combustion Institute*, Vols. 33-2, no. <https://doi.org/10.1016/j.proci.2010.07.018>, pp. 2599-2606, 2011.
- [12] A. Alonso, M. Lázaro, P. Lázaro, D. Lázaro and D. Alvear, "LLDPE kinetic properties estimation combining thermogravimetry and differential scanning calorimetry as optimization targets," *Journal of Thermal Analysis and Calorimetry*, vol. 138, no. <https://doi.org/10.1007/s10973-019-08199-4>, p. 2703–2713, 2019.
- [13] T. A. L. & L. M. S. Hennen, "Numerical Fire Spread Simulation Based on Material Pyrolysis—An Application to the CHRISTIFIRE Phase 1 Horizontal Cable Tray Tests," *Fire*, vol. 3, no. 3, p. 33, 2020.
- [14] K. McGrattan, S. Hostikka, J. Floyd, R. McDermott and M. Vanella, "NIST Special Publication 1018-3 Sixth Edition Fire Dynamics Simulator Technical Reference Guide Volume 3: Validation," NIST, 2022.
- [15] D. F. Specht, "A general regression neural network," *IEEE Transactions on Neural Networks*, Vols. 2-6, p. 568–576, 1991.
- [16] D. Lázaro, E. Puente, M. Lázaro, J. Capote and D. Alvear, "Posibilidades de un modelo sustituto de incendios mediante el empleo de redes neuronales," *Revista Internacional de Métodos Numéricos para Cálculo y Diseño en Ingeniería*, vol. 29 , 2013.
- [17] M. H. M. Beale and H. Demuth, "User's Guide. Deep Learning Toolbox.," MATLAB®, The MathWorks, Inc., 2022.
- [18] K. McGrattan, S. Hostikka, J. Floyd, R. McDermott and M. Vanella, "NIST Special Publication 1019 Sixth Edition Fire Dynamics Simulator User's Guide," NIST, <http://dx.doi.org/10.6028/NIST.SP.1019>, 2022.

ELEVENTH
INTERNATIONAL
SEMINAR



UNDER THE PATRONAGE OF



SAPIENZA
UNIVERSITÀ DI ROMA



**XI
INTERNATIONAL
SEMINAR**

**FIRE AND
EXPLOSION
HAZARDS**

ROME (ITALY)

June 15 – 20, 2025

**Faculty of Civil and
Industrial Engineering**
Sapienza University of Rome